



## Research

**Cite this article:** Deravi LF *et al.* 2014

The structure–function relationships of a natural nanoscale photonic device in cuttlefish chromatophores. *J. R. Soc. Interface* **11**: 20130942.  
<http://dx.doi.org/10.1098/rsif.2013.0942>

Received: 14 October 2013

Accepted: 7 January 2014

### Subject Areas:

biochemistry, biomimetics, biophysics

### Keywords:

reflectin, cephalopod, camouflage, photonics, chromatophores

### Authors for correspondence:

Evelyn L. Hu

e-mail: [ehu@harvard.edu](mailto:ehu@harvard.edu)

Kevin Kit Parker

e-mail: [kkparker@seas.harvard.edu](mailto:kkparker@seas.harvard.edu)

<sup>†</sup>These authors contributed equally to this study.

Electronic supplementary material is available at <http://dx.doi.org/10.1098/rsif.2013.0942> or via <http://rsif.royalsocietypublishing.org>.

# The structure–function relationships of a natural nanoscale photonic device in cuttlefish chromatophores

Leila F. Deravi<sup>1,†</sup>, Andrew P. Magyar<sup>2,†</sup>, Sean P. Sheehy<sup>1</sup>, George R. R. Bell<sup>4</sup>, Lydia M. Mäthger<sup>4</sup>, Stephen L. Senft<sup>4</sup>, Trevor J. Wardill<sup>4</sup>, William S. Lane<sup>3</sup>, Alan M. Kuzirian<sup>4</sup>, Roger T. Hanlon<sup>4</sup>, Evelyn L. Hu<sup>2</sup> and Kevin Kit Parker<sup>1</sup>

<sup>1</sup>Disease Biophysics Group, Wyss Institute for Biologically Inspired Engineering, School of Engineering and Applied Sciences,

<sup>2</sup>School of Engineering and Applied Sciences, and <sup>3</sup>Mass Spectrometry and Proteomics Resource Laboratory, FAS Center for Systems Biology, Harvard University, Cambridge, MA 02138, USA

<sup>4</sup>Marine Biological Laboratory, Program in Sensory Physiology and Behavior, Woods Hole, MA 02543, USA

Cuttlefish, *Sepia officinalis*, possess neurally controlled, pigmented chromatophore organs that allow rapid changes in skin patterning and coloration in response to visual cues. This process of adaptive coloration is enabled by the 500% change in chromatophore surface area during actuation. We report two adaptations that help to explain how colour intensity is maintained in a fully expanded chromatophore when the pigment granules are distributed maximally: (i) pigment layers as thin as three granules that maintain optical effectiveness and (ii) the presence of high-refractive-index proteins—reflectin and crystallin—in granules. The latter discovery, combined with our finding that isolated chromatophore pigment granules fluoresce between 650 and 720 nm, refutes the prevailing hypothesis that cephalopod chromatophores are exclusively pigmentary organs composed solely of ommochromes. Perturbations to granular architecture alter optical properties, illustrating a role for nanostructure in the agile, optical responses of chromatophores. Our results suggest that cephalopod chromatophore pigment granules are more complex than homogeneous clusters of chromogenic pigments. They are luminescent protein nanostructures that facilitate the rapid and sophisticated changes exhibited in dermal pigmentation.

## 1. Introduction

Conformable materials capable of enhancing adaptive coloration in displays are coveted for consumer electronics, camouflaging paints, textiles and cosmetics. Adaptive coloration in cephalopods provides a biological archetype for the design of novel displays, approaching or exceeding the performance of synthetic technologies on most key performance metrics, for example actuation and adaptability to environmental cues [1]. Examination of cephalopods, similar to the cuttlefish *Sepia officinalis*, can elucidate the basic biological, chemical and optical functionalities necessary to provide design rules for novel high-performance colorants required in adaptive, flexible displays.

Cephalopods represent a biological model for flexible displays because of their unique adaptive coloration, enabled principally by the rapid areal expansion and retraction of pigment sacs without a loss of colour fidelity, all within a conformable skin [1–3]. *Sepia officinalis* regulates colour using a vertically arranged assembly of three optical components: the leucophore, a near-perfect light scatterer having uniform reflectivity over the entire visible spectrum; the iridophore, a Bragg stack reflector and the chromatophore, previously considered to be a pigmentary organ acting as a selective colour filter [4–10]. The leucophores and iridophores (both structural elements of coloration) provide an adaptive base layer in the dermal tissue, whereas the chromatophores, located above them, impart an active colour change through areal expansion [11,12]. The chromatophore contains

a multi-scale assembly of nanostructured pigment granules encapsulated within a cell that give rise to its functionality. Each pigment sac contains hundreds of thousands of colorant granules that are highly condensed in the retracted (or punctate) state. Upon expansion, these granules are distributed widely, yet the physical and optical mechanisms that enable each chromatophore to maintain some semblance of uniform colour reflection are unstudied. For example, how are the granules distributed, what minimum thickness of granules is needed to provide relatively uniform coloration and what properties might the granules themselves have to increase the efficiency of reflection?

This paper describes a hierarchical mechanism of coloration within the chromatophore, demonstrating how pigment granules function as nanoscale photonic elements. We hypothesized that chromatophore pigment granules regulate light through absorbance, reflection and fluorescence to produce vivid colours, resulting in uniform coloration during chromatophore expansion. To test our hypothesis, we investigated the structure and function of isolated pigment granules using tandem mass spectrometry and micro-photoluminescence ( $\mu$ PL) spectroscopy, respectively. We found that isolated pigment granules fluoresce between 650 and 720 nm and that this emission correlates with the presence of high-refractive-index proteins, reflectin and crystallin. When the granular structure is altered, the abundance of these proteins is reduced and the emission spectrum is blue-shifted. These data suggest a synergistic role for nanostructure, protein composition and function of pigment granules in regulating the optical performance of chromatophores.

## 2. Material and methods

Experimental methods are described in detail in the electronic supplementary material, SI Materials and Methods; a brief description is included here.

### 2.1. Chromatophore pigment granule extraction, isolation and purification

Adult cuttlefish, *S. officinalis*, (1+ years old) were raised and sacrificed at the Marine Resources Center (MBL, Woods Hole, USA). The whole animal was ethanol washed once prior to sacrifice to minimize microbial/protozoan contamination. Brown chromatophore pigment granules were isolated both from tissue biopsies (dorsal mantle homogenate) and from single cells isolated from dorsal mantle or ventral fin.

A laser-capture microdissection (LCM) system was used to collect individual brown chromatophore pigment cells from *S. officinalis* skin for protein identification. A total of 750 isolated cells from the dorsal mantle and 100 cells from the ventral fin were collected in sterile Eppendorf tubes and stored until further use. Cells were lysed using ultrasonication and purified using sodium dodecyl sulfate-polyacrylamide gel electrophoresis (SDS-PAGE).

### 2.2. Protein purification and analysis using mass spectrometry

SDS-PAGE was used to separate protein fractions from the three conditions. SDS-PAGE on the pigment pellet resulted in multiple protein bands spanning from 0 to 75 kDa. Whole gel lanes were sectioned equally and subjected to tryptic digestion. The resulting peptides were sequenced by tandem mass spectrometry. Peptides

were analysed by microcapillary reverse-phase HPLC, directly coupled to the nanoelectrospray ionization source of an LTQ-Orbitrap Velos or XL mass spectrometer (LCMSMS). Using a custom version of Proteomics Browser Suite (PBS), MS/MS spectra were searched against the NCBI nr protein database and the Molusca subset of NCBI ESTs. Peptide-spectrum matches were accepted with PBS filter sets to attain an estimated FDR of less than 1% using a decoy database strategy.

### 2.3. Denaturation

A previous attempt to denature ommochromes revealed no colour change in response to 20% potassium hydroxide (KOH), suggesting that ommochrome coloration is not affected by strong bases [13]. To determine the effect of proteins, not just the ommochromes, on pigment pellet coloration, we used increasing (0–0.2 M) concentrations of sodium hydroxide (NaOH). NaOH denatures proteins or peptides by hydrolysing amino acid esters or amides, forming carboxylic acids [14]. Similarly, lysed chromatophore cells were denatured overnight, washed and centrifuged three times in normal seawater and analysed.

### 2.4. Analysis of pigment granule denaturation mass spectrometry data

Unique protein release profiles occurring in response to increasing NaOH concentration were identified using Gene Expression Dynamics Inspector (GEDI) software. GEDI provides a map of profiles discovered in the dataset after self-organizing map (SOM) analysis [15]. Proteins observed in the mass spectroscopy datasets were categorized according to their biological function into six primary classes in order to evaluate the effect of NaOH concentration on specific subcomponents of the pigment granules and to reduce the dimensionality of the dataset for visualization purposes. Each tile represents a profile generated from random sampling of the dataset (1000 iterations), where each protein is assigned to the tile with the profile that most closely matches its own (based on Euclidean distance).

### 2.5. Luminescence

Photoluminescence (PL) spectra were collected from two-dimensional isotropic granules on PDMS. Emission spectra under 532 nm laser excitation were measured on a confocal micro-Raman set-up (LabAramis, Horiba) using a 100 $\times$ , 0.95 NA objective. A custom-built microphotoluminescence set-up was used for emission spectra under 410 nm laser excitation and PL excitation measurements.

### 2.6. Absorbance

Absorbance measurements were performed with a UV–Vis spectrometer (DU800 Beckman Coulter) in a 10 mm path length cuvette. Prior to measurement, the pigment granule solution was agitated with a pipette tip to ensure complete suspension of the pigment granules.

### 2.7. Reflectance

Spectral reflectance measurements were obtained using a spectrometer (QE65000, Ocean Optics, Dunedin FL), attached via a 1000  $\mu$ m diameter fibre optic cable to the c-mount of a stereo microscope (Zeiss Discovery V20). Illumination was provided by a high-power broadband xenon light source (HPX2000, Ocean Optics, FL), allowing us to measure reflectance spectra from approximately 400 to 1000 nm (note that our microscope optics block UV wavebands). A diffuse reflection standard (WS-1, Ocean Optics, FL) was used to standardize measurements.

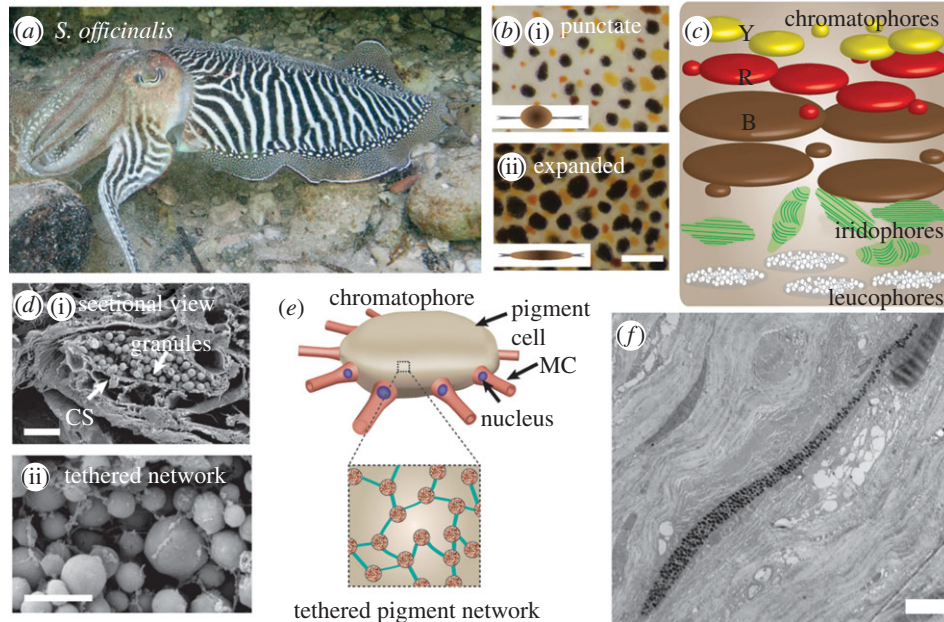


**Figure 1.** Hierarchy of dermal coloration in *S. officinalis*. (a) Adult cuttlefish *S. officinalis*. (b) When actuated, dorsal mantle chromatophores transition from a punctate (i) to an expanded (ii) state in response to visual cues. Scale bar is 1 mm. Inset is a schematic of a punctate and expanded chromatophore in the plane perpendicular to (i) and (ii), respectively. (c) Schematic of the optical units in the cephalopod dorsal mantle. Layering is important in modulating light during actuation. (d) SEM of (i) cross section of chromatophore prepared from wax section. CS is cytoelastic sacculus. Scale bar is 2  $\mu\text{m}$ . (ii) Tethered pigment granules within the chromatophore. Scale bar is 1  $\mu\text{m}$ . (e) Illustration of chromatophore pigment granules tethered within pigment cell anchored by radial muscle cells. (f) Transmission electron micrograph of expanded *S. officinalis* chromatophore, demonstrating that at their radial margins they are often only one granule thick. Scale bar is 4  $\mu\text{m}$ .

## 2.8. Finite difference time domain simulations

A model of the brown chromatophore was built using spheres having a Gaussian distribution fit to the  $528 \pm 68$  nm pigment granule size distribution, as determined from an SEM of brown chromatophores. Pigment granules (approx. 1000) were randomly distributed as a densely packed, non-overlapping system within a  $5 \times 5 \mu\text{m}$  matrix with thickness varied between 1 and 5  $\mu\text{m}$ . For the finite difference time domain (FDTD) simulation (FDTD Solutions, Lumerical), the sidewalls of the cube are set with infinite boundary conditions, and the top and bottom faces are set with perfectly matched layer boundary conditions. The real component of the pigment granules' index of refraction was varied from 1.33 to 1.65. The imaginary portion of the index of refraction was derived from the experimentally measured UV-Vis data for the fully denatured pigment granules from figure 3d. We used this dataset to minimize structural influences on the optical properties (scattering), giving the best approximation of the molecular absorbance of the pigments. Two discrete Fourier transform monitors are placed below and above the granules measuring transmission and reflectance, respectively, and a  $2 \times 2 \times 5 \mu\text{m}$  power monitor is placed at the centre of the granular structure to monitor spatial distribution of absorbance by the pigment granules.

## 3. Results

### 3.1. Cuttlefish chromatophores contain tethered pigment granules

The biophotonic coloration in *S. officinalis* (figure 1a) is regulated by a vertically layered system of pigments and reflectors (figure 1b,c). The uppermost layer in the dermis includes the chromatophores, which are layered yellow over red over brown, with each organ organized in a stellate pattern (figure 1b,c). Chromatophores contain pigment cells, which

expand by the coordinated contractions of the radial muscles (see electronic supplementary material, movie S1), permitting light absorbance and reflectance by the skin over a broad spectral range. Light can interact with all three or fewer of the chromatophore colours depending upon which are expanded. Beneath them in the second layer of the dermis are iridophores, which are Bragg stack reflectors that produce specular structural coloration, primarily of short-wavelength colours that complement the long-wavelength colours of the chromatophores (figure 1c). In the third and bottommost layer are the leucophores (figure 1c), which provide a passive white base layer of diffuse structural coloration upon which the overlying chromatophores and iridophores create patterns in the skin for communication and camouflage. The average maximum reflectance ( $\pm$ s.d.;  $n = 10$ ) from expanded yellow, red and brown cells in the dorsal mantle is  $10 \pm 2\%$  at 580 nm,  $8 \pm 2\%$  at 680 nm and  $12 \pm 1\%$  above 800 nm, respectively (see electronic supplementary material, figure S1a). These data confirm previous findings [3] that chromatophores serve as inverse optical band-pass filters, where shorter wavelengths of light are absorbed by the yellow chromatophores, and longer wavelengths of light are transmitted to and absorbed by the red, then brown chromatophores located deeper within the dermis. This layering enables *S. officinalis* skin to selectively absorb or reflect lights of different colours to accurately perform visual tasks for signalling and camouflage.

Chromatophores are directly innervated (see electronic supplementary material, figure S1b), providing for central nervous system integration of sensory information with motor output regulation of the spatio-temporal skin patterning within hundreds of milliseconds. Coloured responses are enhanced by the anatomical arrangement of pigment granules, which are packed densely within the chromatophores and have

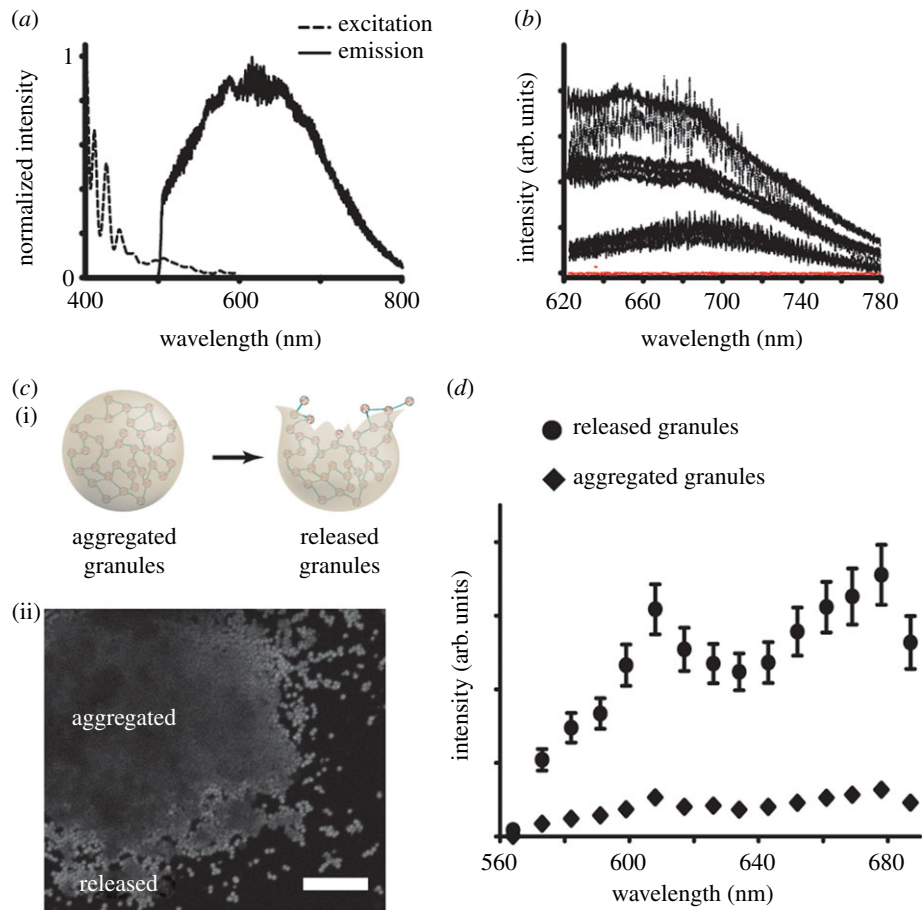


**Figure 2.** Pigment granule luminescence. (a) Optical properties of isolated pigment granules measured using  $\mu$ PL reveal that granules are maximally excited at 410 nm, with an emission maximum centred broadly at 600 nm. (b) Emission intensity (black) for  $n = 10$  individual pigment granules excited at 410 nm. Red line represents emission spectrum for coverslips not coated with pigment granules to show that PDMS autofluorescence does not contribute to luminescence. (c) Chromatophores lysed using focused laser beam. (i) Schematic of lysed chromatophore. (ii) Emission micrograph collected at 680 nm of aggregated and released pigment granules of a lysed brown ventral fin chromatophore excited at 561 nm. Scale bar is 20  $\mu$ m. (d) Variations in luminescence intensity of aggregated and released granules ( $n = 68$ ) excited at 561 nm.

an average diameter of  $528 \pm 68$  nm ( $n = 150$  brown granules). Granules are confined within a cytoelastic sacculus (figure 1d(i)) and are tethered together (figure 1d(ii), illustrated in figure 1e). This system of tethers may help to distribute the pigment granules during chromatophore expansion (figure 1f) to maintain uniform coloration during actuation.

### 3.2. Isolated pigment granules fluoresce in the far-red

Structural coloration is observed in a diversity of animals [16–18], where absorbance is amplified by light scattering among neighbouring nanostructures that have spatial variation in the refractive index on the scale of optical wavelengths [19]. We asked whether pigment granules isolated from *S. officinalis* chromatophores also behave as structural elements of coloration. To test this hypothesis, we measured the structural and optical properties of brown chromatophore pigment granules isolated from the dorsal mantle (details of isolation in the electronic supplementary material, figure S2). Purified pigments were deposited onto a glass coated with polydimethylsiloxane (PDMS) to form isotropic films. Microphotoluminescence ( $\mu$ PL) spectroscopy (see electronic supplementary material, figure S3) was then used to characterize the optical properties of individual granules. An excitation sweep over the granules produced a local excitation maximum at 410 nm with the secondary peak at 505 nm (figure 2a). When

excited at 410 nm, granules exhibited a broad emission maximum centred between 650 and 720 nm (figure 2b). The precise emission wavelength varied as a function of focal plane for individual granules, which suggests a non-uniform distribution of emitters.

Given the extensive optical characterization of chromatophores in past studies [3–5,7–9], it is noteworthy that this far-red emission had not been reported previously in cephalopods. Recently, a similar fluorescence signal, peaking around 595 nm, was observed in fish chromatophores, which are very different cell types despite the same name [20]. We reasoned that luminescence intensity is dependent on granule aggregation within the chromatophore. To test this, *in situ* luminescence of brown chromatophores isolated from the dorsal mantle (figure 2c(i)) was measured using  $\mu$ PL and laser-scanning confocal microscopy. We observed that the luminescence intensity of aggregated granules within an intact cell is nearly  $6\times$  lower than the intensity of granules released from lysed cells, suggesting that aggregation reduces luminescence (figure 2c(ii), measured in figure 2d). We reason that fluorescence is diminished owing to increased re-absorption processes in the aggregated material, where a photon is emitted by the pigment granule, but scatters among other granules before it is finally absorbed by pigment molecules. The compacted chromatophore represents a net higher effective refractive index, resulting in increased photon

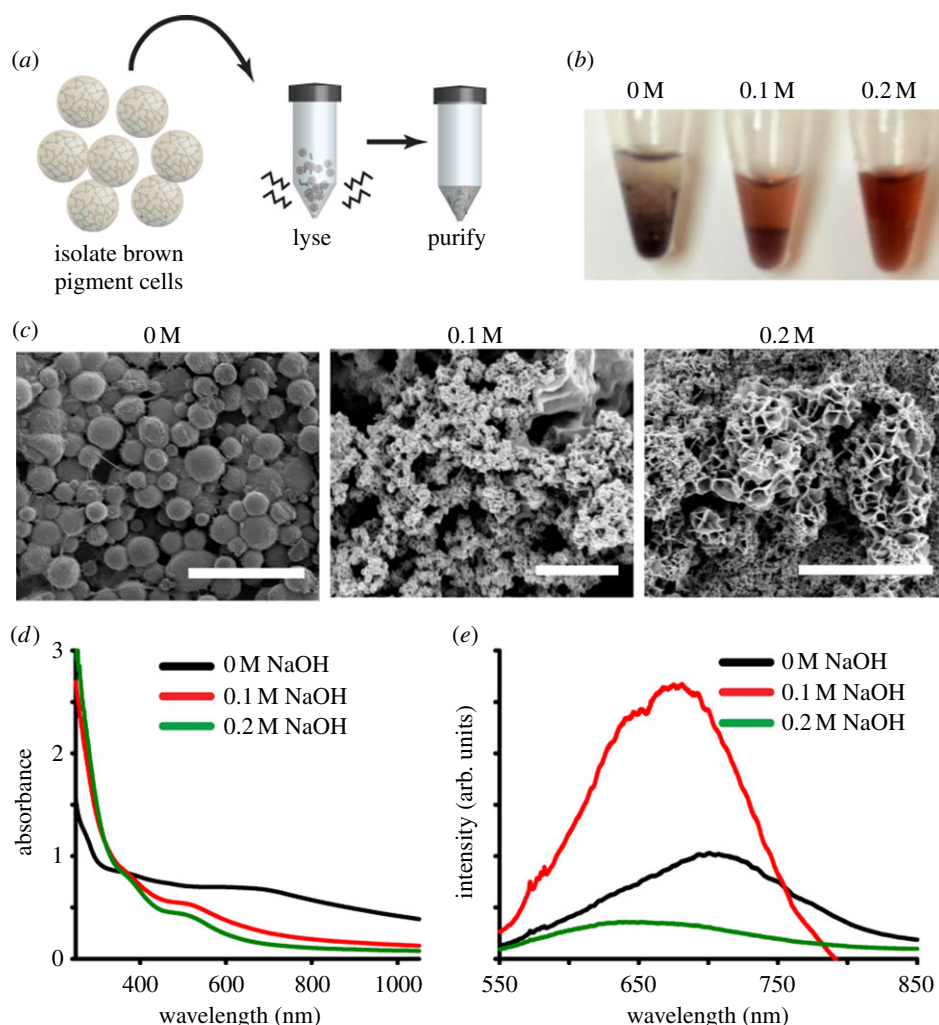


**Figure 3.** Contribution of granular structure to optical properties of pigment granules. (a) Schematic of pigment granule isolation. Single brown pigment cells are isolated from the dorsal mantle, lysed via ultrasonication and purified using centrifugation and washing. (b) Bulk coloration from a complete pigment extract is altered in the presence of increasing NaOH concentration. (c) SEM of denatured granules shows correlation between loss in granular morphology and coloration. Scale bar is 5  $\mu\text{m}$ . (d) Visible absorbance decreases, as ultrastructure is disrupted with increasing NaOH. (e) Luminescence blue-shifts as the granule structure are destroyed.

scattering and a net increase in the effective path length of light through the chromatophore, thereby increasing the probability that photons are absorbed. To investigate this relationship between packing density and luminescence, released granules were dehydrated to form a free-standing film composed of densely packed, overlapping pigment granules (see electronic supplementary material, figure S4a). Luminescence across the film was measured (see electronic supplementary material, figure S4b,c) and compared to the emission intensity of a dispersed, isotropic monolayer, where granules are separated by more than a wavelength of light (see electronic supplementary material, figure S4d). Variations in emission intensity between the two conditions suggest that the packing density of granules regulates luminescence (see electronic supplementary material, figure S4e,f). The presence of luminescence at larger intergranular separations (such as in a fully expanded chromatophore) could provide a mechanism to maintain colour richness for fully expanded, lower granule-density chromatophores.

### 3.3. Chromatophores are composed of high-refractive index proteins

Pigments in brown chromatophores of cephalopods have been identified as ommochromes [21], which are a class of small-molecule metabolites derived from tryptophan [22,23].

Depending on their oxidation state, ommochromes can have a brown–black colour with an absorption maximum at 525 nm [24] and an emission maximum centred around 450–475 nm [25,26]—both of which are blue-shifted from the absorption and luminescence maxima of the brown chromatophore pigment granules reported here. Because of these spectral differences, we asked whether pigment granules are composed of more than ommochromes. We investigated the protein composition of lysed, chromatophore layer homogenate as well as individual laser capture microdissected chromatophores using tandem mass spectrometry (see electronic supplementary material, tables S1–S3). To mitigate contaminations from the adjacent leucophore or iridophore tissue, we focused on extracting single brown chromatophores from the dorsal mantle using laser-capture microdissection. These data show that reflectin and crystallin isoforms are the primary components of the isolated chromatophores.

To determine whether the contribution of reflectins enhances the optical properties of pigment granules, we used increasing concentrations of sodium hydroxide (NaOH) to denature granules purified from isolated chromatophores (figure 3a). NaOH hydrolyses and cleaves esters and amides from both proteins and small molecules, breaking down primary protein structure [27]. Thus, if the granules contain proteins then NaOH treatment would disrupt their structure

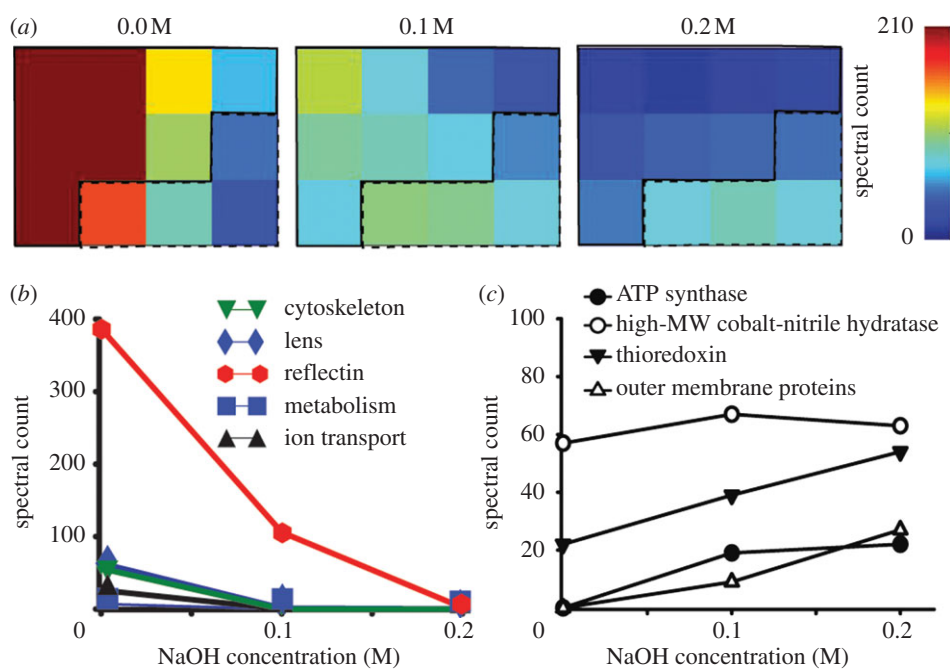


**Figure 4.** Tandem mass spectrometry used to analyse proteins that are released from granules upon denaturation. (a) Illustration of patterns in the protein dataset as a function of increasing NaOH using GEDI software. GEDI represents all different release profiles and organizes them based on their similarity to one another, providing a visual representation of change in both the shape and magnitude of protein content over the concentration series. Proteins previously unreported from cephalopods fell within the tiles bound by the dashed lines in the mosaic. (b) Cluster assignment map of cephalopod protein denaturation profiles from laser isolated brown chromatophores. (c) Spectral count profiles of proteins previously unreported from cephalopods (represented by the dashed line in (a)) do not vary substantially as a function of increasing NaOH.

and function. We observed that the visible colour of the granules was altered with increasing concentrations of NaOH, shifting the supernatant colour from dark brown to red (left to right, figure 3b). This variation in colour correlated with a change in granular ultrastructure (figure 3c) suggests that visible colour is influenced by the nanostructure of the pigment granules. Absorbance in the visible range decreased as a function of increasing NaOH concentration (figure 3d), indicating that the loss of structure reduced the degree of light scattered through the solution. Luminescence intensity, however, initially increased after 0.1 M NaOH treatment (figure 3e, red line), which may have been associated with the highly altered ultrastructure of the pigment granules observed in SEM (figure 3c). After 0.2 M NaOH treatment (figure 3e, green line), granule luminescence intensity decreased significantly, correlating with the degradation of granular structure. These data show that the emission wavelengths of granules treated with 0.1 M and 0.2 M NaOH are blue-shifted when compared with the untreated granules, suggesting that NaOH exposure destroys the ability of granules to emit at far-red wavelengths.

Variations in granule composition were measured as a function of increasing NaOH using tandem mass spectrometry (figure 4a, electronic supplementary material, table S1). The sensitivity of proteins to NaOH was used to categorize and cluster the proteins that constitute the pigment granules (see electronic supplementary material, figure S5). We observed two distinguishable trends in protein abundance from the denaturation experiments (figure 4). First, putative cephalopod proteins, such as reflectins, lens, cytoskeleton, ion-transport and metabolism-related proteins, all decreased with increasing NaOH (figure 4b). Second, proteins previously unreported from cephalopods remained constant with NaOH (figure 4c, electronic supplementary material, table S1). Proteins that follow the second trend include thioredoxin and cobalt-nitrile

hydratase—both are identical to bacterial proteins present in *Escherichia coli* and *Actinobacteria*, respectively. Given that cephalopods have abundant microbial fauna on their skin surface, we were unable to fully prevent microbes being partially mixed with isolated chromatophore tissues. Data from the proteomics analysis coupled with electron microscopy (figure 3c) are consistent with the concept that reflectin and crystallin are structural components of the chromatophore pigment granule and that these proteins contribute to absorbance and luminescence.

### 3.4. Pigment granules are effective absorbers of light

To better understand how pigment granules themselves absorb or scatter light, a model chromatophore containing a 5  $\mu\text{m}$  cube of densely packed pigment granules was constructed *in silico* (see electronic supplementary material, figure S6(i,ii)). Reflectins have an index of refraction as high as 1.59 [28], which provide important guidance in defining the model parameters. The amount of reflected light from the pigment granules packed within the cube was calculated using FDTD simulations (Lumerical, FDTD Solutions) [14]. FDTD Solutions is a complete Maxwell solver providing numerical solutions for three-dimensional electromagnetic fields and was used to determine the role of pigment refractive index and granular structure on chromatophore absorbance over a wide frequency range. Pigment refractive index within the simulated chromatophores was varied from 1.33 to 1.65 (see electronic supplementary material, figure S6(iii)). Our comparison between the simulation and experimentally measured reflectivity from brown ventral fin chromatophores (see electronic supplementary material, figure S6(iii), black line) suggests that, similar to reflectin, the granules have a refractive index greater than 1.5.

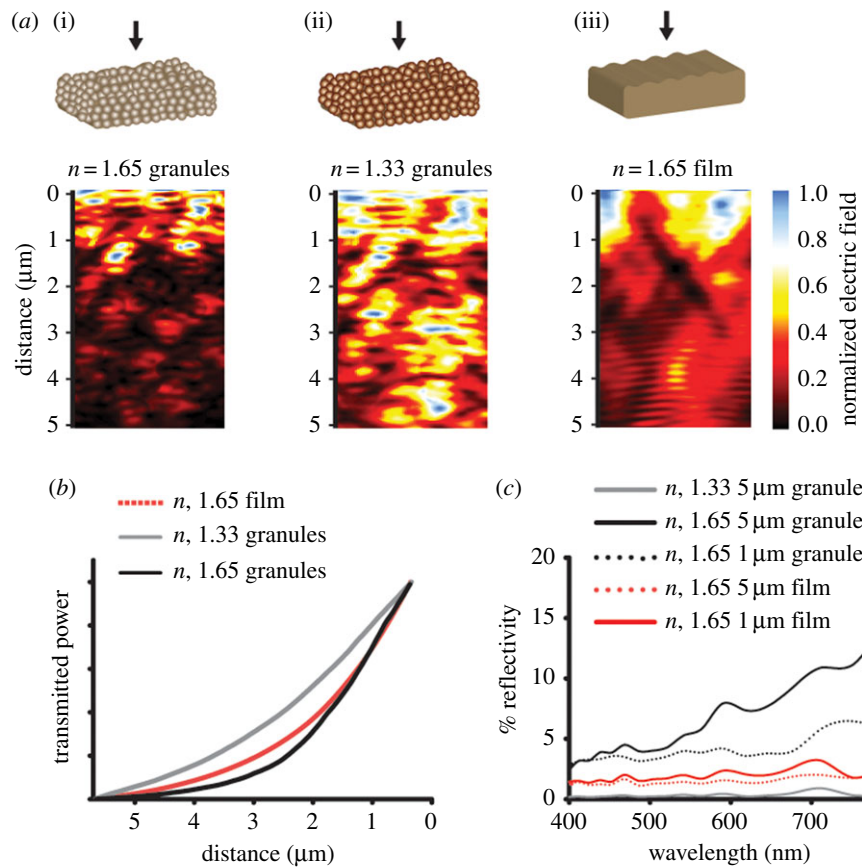


**Figure 5.** FDTD simulations indicate that thinner layers of high-index granules more effectively attenuate incident light than low-index granules or a roughened film. (a) Strength of electric fields as a function of simulated chromatophore structure and path length where (i), (ii), and (iii) represent a high-index granular ‘chromatophore’, low-index granular ‘chromatophore’ and a high-index non-granular ‘chromatophore’, respectively. Arrow indicates the direction of illumination by a plane-wave source. (b) Normalized transmitted power as a function of ‘chromatophore’ thickness. The lowest transmitted power from high-index granules means that the incident light is more greatly absorbed by the granular structure. (c) Reflectivity as a function of refractive index, thickness and granularity indicating that high-index granular structures result in higher reflectivity than non-granular films of the same thickness.

To determine whether pigment granularity enhances reflectivity, the intracellular morphology of the model chromatophore was varied from a densely packed granular structure with refractive indices of either 1.33 or 1.65 to a non-granular, homogeneous film with a refractive index of 1.65 (figure 5a). The non-granular film was modelled with a surface roughness similar to that of the granular structure. For the three structures, there are clear differences in the intensity of the normalized electric field (i.e. light) as a function of depth. The simulated data of figure 5a can be used to calculate an absorbance length through the material, extracted from the exponential decay of the transmitted power through each structure (figure 5b). Larger absorbance lengths indicate less effective absorbance of incident light. The high-index granular structure exhibited the shortest absorbance length (1.1 μm, figure 5a(i)), while the low-index granular structure (2.9 μm, figure 5a(ii)) and the rough film (1.7 μm, figure 5a(iii)) required more depth to attenuate the same amount of light. The model predicted that high-index granular pigments enhance the scattering of the incident light within the chromatophore, thereby increasing the effective path length that light experiences as it passes through the chromatophore. Consequently, light has more opportunities to interact with pigments, thus a higher probability of being absorbed. The enhanced absorbance is particularly important when placed in context with the 500% change in chromatophore surface area that often produces a pigment layer fewer than three granules thick when expanded (figure 1f). As our model chromatophore decreases

in thickness (figure 5c), there is initially little change in the per cent reflected power until the chromatophore becomes less than 2 μm thick (see electronic supplementary material, figure S7). These data suggest that the low absorbance length of high-index granular structures enhances chromatophore coloration during actuation.

## 4. Discussion

Our data suggest that visible coloration in the *S. officinalis* chromatophore is facilitated by the nanostructure and composition of the pigment granules themselves. This hierarchy enables the cuttlefish to produce a wide variety of body patterns that function in signalling displays or camouflage. An additional feature of the chromatophore is pigment granule luminescence, which, in addition to the already known absorbance, may contribute to the colour intensity and hue of the expanded chromatophores and, as in reef fish [20], could be used for signalling. The presence of reflectin, along with the observed difference in luminescence between ommochromes and intact granules, indicates that *S. officinalis* pigment granules are more complex bionanophotonic devices than previously known.

To date, chromatophore function has been characterized by the selective absorption of light by ommochrome pigments. Our finding that granules contain significant amounts of the high-refractive-index protein reflectin is important because

reflectins are associated with the production of structural coloration in cephalopod iridophores [15,29,30] and leucophores [10]. For the first time, these proteins have been found in a cephalopod chromatophore, which has classically been deemed a pigmentary organ. The differences in spectral properties between pure ommochromes and intact chromatophore granules, together with the presence of reflectins and crystallins observed in our protein composition analysis, suggests that *S. officinalis* pigment granules are composed of more than just ommochromes.

The tethering system reported here suggests that chromatophores maintain an adaptable granule distribution. The tether network architecture also may directly regulate chromatophore absorption and fluorescent emission through control of pigment granule dispersal. The protein content of the tethering is unknown. What is known is that the network is physically connected, via the cytoelastic sacculus, to the external musculature. This structural hierarchy enables rapid geometrical distortion of the chromatophore, resulting in the redistribution of the optically and mechanically coupled granules.

The robust optical properties and network architecture of *S. officinalis* chromatophores make them a compelling model for the bioinspired design of new types of pigments and

photonic devices for conformable displays. The use of high-refractive-index granules to enhance absorbance can provide improved colour fidelity with a thinner form factor. In contrast to camouflage technologies that rely on pixilation to disrupt pattern recognition, a layered, nanogranular structure, similar to a cephalopod chromatophore, provides enhanced colour contrast. The design features gleaned from these studies provide intriguing insights into the development of artificial photonic systems with a wide spectral response owing to the collection of ambient light using packaged photonic granules.

**Acknowledgements.** The authors gratefully acknowledge the use of facilities at the Harvard Center for Nanoscale Systems and the Wyss Institute for Biologically Inspired Engineering. We also acknowledge Mr T.-L. Liu for his assistance with electronic supplementary material, figure S3 and B. Budnik, R. Robinson and J. Neveu for expert assistance with mass spectrometry.

**Funding statement.** This work was partially funded by the Defense Advanced Research Projects Agency CINAPSE (W911NF-10-1-0113 for K.K.P., E.L.H., R.T.H.), Harvard University Nanoscale Science and Engineering Center supported by the National Science Foundation (PHY-0646094 for K.K.P.), Harvard University Materials Research Science and Engineering Center supported by the National Science Foundation (DMR-0213805 of K.K.P.) and AFOSR grant FA9550-09-0346 to R.T.H.

## References

- Kreit E, Mäthger LM, Hanlon RT, Dennis PB, Naik RR, Forsythe E, Heikenfeld J. 2012 Biological vs. electronic adaptive coloration: how can one inform the other? *J. R. Soc. Interface* **10**, 20120601. (doi:10.1098/rsif.2012.0601)
- Hanlon RT, Messenger JB. 1996 *Cephalopod behaviour*. Cambridge, UK: Cambridge University Press.
- Mäthger LM, Hanlon RT. 2007 Malleable skin coloration in cephalopods: selective reflectance, transmission and absorbance of light by chromatophores and iridophores. *Cell Tissue Res.* **329**, 179–186. (doi:10.1007/s00441-007-0384-8)
- Sutherland RL, Mäthger LM, Hanlon RT, Urbas AM, Stone MO. 2008 Cephalopod coloration model. I. Squid chromatophores and iridophores. *J. Opt. Soc. Am.* **25**, 588–599. (doi:10.1364/JOSAA.25.000588)
- Cloney RA, Brocco SL. 1983 Chromatophore organs, reflector cells, iridocytes and leucophores in cephalopods. *Am. Zool.* **23**, 581–592.
- Hanlon RT, Messenger JB. 1988 Adaptive coloration in young cuttlefish (*Sepia officinalis* L)—the morphology and development of body patterns and their relation to behavior. *Phil. Trans. R. Soc. Lond. B* **320**, 437–487. (doi:10.1098/rstb.1988.0087)
- Mäthger LM, Denton EJ, Marshall NJ, Hanlon RT. 2009 Mechanisms and behavioural functions of structural coloration in cephalopods. *J. R. Soc. Interface* **6**, S149–S163. (doi:10.1098/rsif.2008.0366.focus)
- Sutherland RL, Mäthger LM, Hanlon RT, Urbas AM, Stone MO. 2008 Cephalopod coloration model. II. Multiple layer skin effects. *J. Opt. Soc. Am.* **25**, 2044–2054.
- Mäthger LM, Roberts SB, Hanlon RT. 2010 Evidence for distributed light sensing in the skin of cuttlefish, *Sepia officinalis*. *Biol. Lett.* **6**, 600–603. (doi:10.1098/rsbl.2010.0223)
- Mäthger LM *et al.* 2013 Bright white scattering from protein spheres in color changing, flexible cuttlefish skin. *Adv. Funct. Mater.* **23**, 3980–3989. (doi:10.1002/adfm.201203705)
- Florey E. 1969 Ultrastructure and function of cephalopod chromatophores. *Am. Zool.* **9**, 429–442.
- Florey E, Kriebel ME. 1969 Electrical and mechanical responses of chromatophore muscle fibers of squid, *Loligo opalescens*, to nerve stimulation and drugs. *Z. Vergleichende Physiologie* **65**, 98–130. (doi:10.1007/BF00297991)
- Van den Branden C, Gillis M, Richard A. 1980 Carotenoid producing bacteria in the accessory nidamental glands of *Sepia officinalis*. *Comp. Biochem. Physiol. B Biochem. Mol. Biol.* **66**, 331–334.
- Gedney SD. 2011 *Introduction to the finite-difference time-domain (FDTD) method for electromagnetics*. Morgan & Claypool.
- Holt AL, Sweeney AM, Johnsen S, Morse DE. 2011 A highly distributed Bragg stack with unique geometry provides effective camouflage for Loliginid squid eyes. *J. R. Soc. Interface* **8**, 1386–1399. (doi:10.1098/rsif.2010.0702)
- Fox DL. 1953 *Animal biochromes and structural colours*, pp. 379. London, UK: Cambridge University Press.
- Parker AR. 1999 Invertebrate structural colours. In *Functional morphology of the invertebrate skeleton*. (ed. E Savazzi), pp. 65–90. London, UK: John Wiley & Sons.
- Prum RO, Cole JA, Torres RH. 2004 Blue integumentary structural colours in dragonflies (Odonata) are not produced by incoherent Tyndall scattering. *J. Exp. Biol.* **207**, 3999–4009. (doi:10.1242/jeb.01240)
- Vukusic P, Sambles JR, Lawrence CR. 2004 Structurally assisted blackness in butterfly scales. *Proc. R. Soc. B* **271**, S237–S239. (doi:10.1098/rsbl.2003.0150)
- Wucherer MF, Michiels NK. 2012 A fluorescent chromatophore changes the level of fluorescence in a reef fish. *PLoS ONE* **7**, e37913. (doi:10.1371/journal.pone.0037913)
- Butenandt A, Schäfer W. 1962 Ommochromes. In *Recent progress in the chemistry of natural and synthetic coloring matters and related fields* (ed. TS Gore), pp. 13–33. New York, NY: Academic Press.
- Elofsson R, Kauri T. 1971 Ultrastructure of chromatophores of *Crangon* and *Pandalus* (Crustacea). *J. Ultrastructure Res.* **36**, 263–270. (doi:10.1016/S0022-5320(71)80103-X)
- Insausti TC, Casas J. 2008 The functional morphology of color changing in a spider: development of ommochrome pigment granules. *J. Exp. Biol.* **211**, 780–789. (doi:10.1242/jeb.014043)
- Dontsov AE, Fedorovich IB, Lindstrom M, Ostrovsky MA. 1999 Comparative study of spectral and antioxidant properties of pigments from the eyes of two *Mysis relicta* (Crustacea, Mysidacea) populations,

- with different light damage resistance. *J. Comp. Physiol. B Biochem. Syst. Environ. Physiol.* **169**, 157–164. (doi:10.1007/s003600050206)
25. Yagi S, Ogawa H. 1996 Effect of tryptophan metabolites on fluorescent granules in the Malpighian tubules of eye color mutants of *Drosophila melanogaster*. *Zool. Sci.* **13**, 97–104. (doi:10.2108/zsj.13.97)
  26. Van den Branden C, Declair W. 1976 A study of the chromatophore pigments in the skin of the cephalopod *Sepia officinalis*. *Biologische Jaarb* **44**, 345–352.
  27. Hamaguchi K. 1955 Studies on protein denaturation by surface chemical method. 2. On the mechanism of surface denaturation of lysozyme. *J. Biochem.* **42**, 705–714.
  28. Kramer RM, Crookes-Goodson WJ, Naik RR. 2007 The self-organizing properties of squid reflectin protein. *Nat. Mater.* **6**, 533–538. (doi:10.1038/nmat1930)
  29. Crookes WJ, Ding LL, Huang QL, Kimbell JR, Horwitz J, McFall-Ngai MJ. 2004 Reflectins: the unusual proteins of squid reflective tissues. *Science* **303**, 235–238. (doi:10.1126/science.1091288)
  30. Andouche A, Bassaglia Y, Baratte S, Bonnaud L. 2013 Reflectin genes and development of iridophore patterns in *Sepia officinalis* embryos (Mollusca, Cephalopoda). *Dev. Dyn.* **242**, 560–571. (doi:10.1002/dvdy.23938)